Springer

KSME

Journal of Mechanical Science and Technology 33 (4) (2019) 1817~1831
www.springerlink.com/content/1738-494x(Print)/1976-3824(Online)
DOI 10.1007/s12206-019-0334-x

Laser beam machining of zirconia ceramic: An investigation of micro-machining geometry and surface roughness †

Basem M. A. Abdo[1,2,*], Naveed Ahmed[2,3], Abdulaziz M. El-Tamimi[1], Saqib Anwar[1], Hisham Alkhalefah[2] and Emad Abouel Nasr[1,4]

[1]*Industrial Engineering Department, College of Engineering, King Saud University, Riyadh, 11421, Saudi Arabia*
[2]*Princess Fatima Alnijiris's Research Chair for Advanced Manufacturing Technology (FARCAMT Chair), Advanced Manufacturing Institute, King Saud University, Riyadh, Saudi Arabia*
[3]*Department of Industrial and Manufacturing Engineering, University of Engineering and Technology, Lahore, Pakistan*
[4]*Faculty of Engineering, Mechanical Engineering Department, Helwan University, Cairo 11732, Egypt*

(Manuscript Received September 10, 2018; Revised November 28, 2018; Accepted December 11, 2018)

Abstract

Micro-machining of dental ceramics namely as zirconium oxide is carried out through laser beam machining. Micro-channels of different sizes are fabricated under different laser parameters. The laser process performance is evaluated by considering the geometrical and quality responses associated with micro-channels. Laser intensity, pulse frequency, scanning speed and layer thickness per laser scan are opted as the influential controlling parameters. Geometrical characteristics of micro-channels include upper width (W_U), lower width (W_L), depth (D), taper angle of micro-channel's sidewalls at right side (θ_R), and taper angle at left side (θ_L). Quality of the machined micro-channels is evaluated by means of surface roughness (R_a) of the bottom surface. Effects of each of the laser parameters on each of the geometrical and quality responses are studied in order to get the influential trends of laser parameters. SEM analysis is further performed to assess the micro-details of machining results. The results reveals that the shape and size of micro-channel are very sensitive to the variation in laser parameters. Two types of micro-channels shapes are obtained having V-shaped and U-shaped cross-sections. Furthermore, it is quite challenging to achieve the micro-channels with reasonable amount of lower width (W_L).

Keywords: Ceramics; Laser; Machining; Micro-channels; Scan; Speed; Surface roughness; Zirconia

1. Introduction

Advanced ceramics such as alumina, zirconia, aluminum nitride, and silicon nitride etc. are extensively being used in various applications which can be found in nuclear industry, aerospace industry, bioengineering, biomedical implants, dentistry, and automotive industry. All this is mainly possible due to having unique combinations of properties which include very high hardness, excellent wear resistance, and chemical inertness [1]. However, the same set of properties are attractive for the said applications in one end but the darker side of these ceramics is that they create challenges with their machining. Additionally, fabrication of micro-features in these ceramics is more challenging. Furthermore, micro-electro-mechanical systems (MEMS) devises are widely used in different industrial sectors such as for gas sensors operating in harsh environment. Fabrication of MEMS devises require a platform onto which the micro-features are fabricated according to the desired requirements.

Zirconia oxide, one of the advanced ceramic materials, has one of the applications in the form of MEMS platforms as well. Zirconia dental ceramic is a material extensively used in various dental applications such as dental implants and dental restoration. These application require fabrication of micro-features such as microchannels in such materials. Such platforms can also be used for other MEMS devises such as used for fast thermometers, bolometric matrices and flow meters [2]. Micro-features to be manufactured on such platforms could be micro-channels, micro-membrane, and micro-holes [3]. For example, micro-channels are used in the design of biomedical scaffolds made of ceramics where bone generation in micro-channels carried out by the bone marrow absorption through capillary action [4, 5]. Development of micro-channels in membranes of different ceramics and composites are also required in different filtration systems such as photo-catalytic filtration [6].

Micro-channels and other similar micro-features are almost

*Corresponding author. Tel.: +966 509250307, Fax.: +966 1 4693788
E-mail address: babdo@ksu.edu.sa, ORCID: 0000-0002-7003-7453
† Recommended by Associate Editor Yongho Jeon

impossible to generate in ceramics through conventional machining processes but with nonconventional ones. Abrasive slurry jet machining can be used to machine micro-channels in ceramics. Kowsari [7] employed abrasive water jet to fabricate micro-channels in aluminum nitride, alumina, and zirconium in order to study the widths, depths and shapes of micro-channels. Non-conductive nature of the zirconium oxide imparts limitations on some of the non-conventional processes as well, especially the processes based on electrical conductivity such as electric discharge machining (EDM) and electro-chemical machining (ECM) [8]. However, this difficulty can somehow overcome by introducing assisting electrodes of conductive materials in the form of a conductive coating or cementing conductive films of the machining surface of zirconia oxide [9, 10]. Laser beam machining is one of the alternative non-conventional machining processes offering a wide range of flexibilities such as the laser process does not require complex tools and offers flexibilities in electrical conductivity, hardness and toughness of the machining materials. Laser beam machining of ceramics is, however, studied in different perspectives but not fully explored and needs much research in future. Laser assisting machining (LAM) is however widely investigated for ceramics [11] and metals [12]. For example, Kim and Lee [13] and Kim [14] investigated the LAM performance while milling and turning silicon nitride assisted with preheating by laser. Laser preheating in front of the milling/turning tool is experienced to be highly effective in controlling the machining performance. The decrease in tool wear and cutting force and reductions in catastrophic tool failures are the prominent advantages obtained through LAM. Kizaki [15] assessed the effectiveness of laser assistance while grinding zirconia using the diamond tool. It has been found that the laser assistance effectively reduced the grinding force and tool damage. Similarly, laser thermal shocks assist the grinding process and significantly reduce the grinding force and energy while finishing the zirconia surface [16].

Laser direct writing or machining of zirconia is not very commonly studied especially for micro-machining purposes. Since during laser machining many physical phenomena act simultaneously and influence the machining results. Therefore, it is very difficult to understand the real effects of the individual control parameter. However, it has been found that the performance of the laser machining process strongly depends on the pulse duration of the laser beam especially when dealing with ceramics like zirconia oxide. Millisecond lasers offer high cutting rates due to high energy available because of long pulse duration. The quality of the finished surface is therefore limited due to heavy re-deposited melt within the machining area. In contrast to this, a shorter pulse duration as offered by nanosecond lasers offers good surface quality but longer machining time [17]. Millisecond pulse duration also induces a significant amount of recast layer and crack propagation during laser drilling and milling [18]. Propagation of the micro-cracks while machining zirconia is mainly due to the thermal expansion rate and material absorption. Regarding controlling the machining depth during laser machining of structural ceramics, the energy absorption plays an important role. Energy absorptivity transitions depend on the rise in temperature during different stages of the laser machining [19]. Nanosecond, as well as picosecond lasers, almost have similar results in terms of machining rate during laser beam machining of zirconia. However, the micro-machining of zirconia through picosecond laser machining revealed that the machining results regarding surface topography are superior compared with nanosecond laser. Picosecond regime also allows getting zirconia surfaces with no evidence of micro-cracking [20]. Dear [18] proposed that nanosecond pulsed laser could be a promising alternative to avoid the poor machining performance of laser machining of zirconia. Noda [21] treated zirconia surfaces by Nd:YAG dental laser and analyzed the surface modifications. They stated that the dental laser damages the Zirconia surface in the form of micro-structural change and reduction in the content of Oxygen at the surface which accumulatively reduces the mechanical strength.

Other than pulse duration, many laser parameters are having the effect on machining. Milling of zirconia through Yb:YAG fiber laser has revealed that the material removal rate is strongly dependent on scanning speed and hatch distance [22]. It has also been claimed that the roughness of the milled surface of zirconia severely affected by scan speed and hatch distance. Higher values of scan speed, number of repetitions and hatch distance imparts poor surface roughness. Likewise, the pulse rate directly influences the surface roughness of laser machined structural alumina. High pulse rate produces the alumina surface with high roughness [23]. Similar results have also been reported while micro-machining the structural ceramic alumina. In another study, it has been claimed that the laser parameters including laser intensity, pulse overlap and pulse frequency directly controls the surface topography of the milled surface [24]. An increase in lateral overlap of the laser scans causes the surface roughness of the ceramics to be high [25].

In this present research an attempt has been made to machine zirconia by Nd:YAG laser beam machining operating with 1064 μm wavelength and pulse duration of 10 μs. Micro-channels have been machined, and the process performance is evaluated by studying the micro-channel geometry and surface roughness of the micro-channels' inner surfaces. Process responses regarding micro-channel geometry include upper width, lower width, depth, and taper angles at both sides of micro-channel sidewalls, whereas, the surface roughness of the bottom surface is considered as the quality response of the laser beam machining. The influences of each of the predominant laser process parameters (laser intensity, pulse frequency and scanning speed, and layer thickness) on each of the six responses are categorically examined to understand the parametric trends over the micro-channels' geometrical contents. The micro-channels profiles and surface quality are further discussed in detail with the help of scanning electron microscopic analysis. It should be noted that zirconia dental ceramic is extensively used in various dental applications such as den-

tal implants and dental restoration. These applications often require fabrication of micro-features such as microchannels with high dimensional accuracy and good surface quality. The current study provides a detailed investigation of the Nd:YAG laser pulsed micro-channeling of zirconia.

2. Materials and methods

Yttria Stabilized Zirconia Oxide (ZrO2-Y2O3) has been used as a substrate material for micro-machining from Ceram-Tec Germany. All the zirconia dental samples used in the experiments were of the dimension 50 mm × 50 mm ×10 mm. Chemical composition and thermos-mechanical properties of zirconia oxide as per manufacturer [26] are presented in Tables 1 and 2, respectively. Different sized micro-channels has been machined through laser beam milling. Lasertec 40 from DMG Mori Seiki is used throughout the experimentation. Lasertec 40 is used with its by-default basic settings such as laser beam, wavelength, pulse mode, spot size and power etc. The basic details of laser equipment/machine parameters are such as it consists of continuous wave (CW) pulsed Nd:YAG laser with 1064 nm wavelength. The laser beam of spot size 30 µm produced as a result of a train of pulses with 10 µm pulse duration and follow the Gaussian mode. The laser with spot size of 30 µm has maximum power of 30 W which produces 42.441 kW/mm^2 laser intensity. Fractions (in the form of percentage) of maximum power or laser intensity is utilized depending upon the requirements of desired material removal rate.

Micro-channels having two types of cross-sectional area are fabricated including square cross-section (width x depth = 500 µm x 500 µm) and rectangular cross-section (width x depth = 500 µm x 800 µm). Experimentation has further been divided for each of the two types of micro-channels in such a way that 36 experimental runs are performed for square cross-sectional micro-channels, and 24 experiments are carried to produce rectangular cross-sectional micro-channels. Laser intensity, pulse frequency and laser scanning speed was considered as the control factors which mainly control the machining geometry during laser beam machining. On the other hand, laser scanning track displacement and laser focus point were kept constant. Track displacement also called as the distance between two successive laser scans was kept at 10 µm whereas focus point of the laser spot was fixed at the top surface of the workpiece. The thickness of the layer to be removed by one laser scan plays an important role in laser beam machining. Selection of appropriate value of layer thickness (the desired depth of cut per laser scan) is a complex process. Layer thickness of 2 µm is recommended by the machine manufacturer. However it may or may not be suitable for every material. The ranges of the laser process parameters were selected based on the manufacturer recommendation and previous studies reported on laser machining of similar bio-materials [22, 27-30]. Then, preliminary experiments were performed to decide the actual levels of the process parameters that were later used to conduct the final set of experiments.

Table 1. Chemical composition of zirconia oxide.

Elements	Unit	Value
$ZrO_2 + HfO_2 + Y_2O_3$	%	≥ 99.0
Y_2O_3	%	4.5 - 5.6
HfO_2	%	1.8 - 2.2
Al_2O_3	%	0.03 - 0.07
Other oxides	%	≤ 0.5
Chemical solubility	µg/cm^2	≤ 100

Table 2. Mechanical and thermal properties of zirconia oxide.

Property	Unit	Value
Flexural strength (4-point bending)	MPa	1100
Flexural strength (3-point bending)	MPa	1200
Vickers hardness	HV 0.5	1250
Young's modulus	GPa	210
Thermal expansion coefficient WAK 20-600 °C	10-6 K-1	10.7
Density	g/cm^3	≥ 6.07
Grain size	-	≤ 0.40

Table 3. Experimentation plan for micro-channel machining of dental ceramic.

Channel size	Channel shape (cross-sectional)	Laser parameters					Exp. runs
		Layer thickness; LT (µm)	Track displacement; TD (µm)	Laser intensity; I (%)	Pulse frequency; f (kHz)	Laser scanning speed; v (mm/s)	
Width: 500 µm Depth: 500 µm Length: 6 mm	Square	2	10	75	5	25	36
				80	10	50	
				85	15	75	
				90	20	100	
Width: 500 µm Depth: 800 µm Length: 6 mm	Rectangle	4	10	87	5	100	24
				90	8	200	
				93	11	300	
				96	15	400	

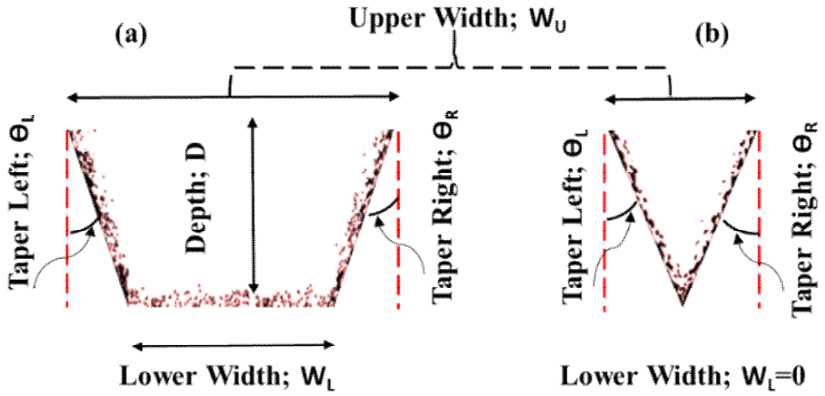

Fig. 1. Schematic diagram of micro-channels: (a) Trapezoidal x-section; (b) conical x-section.

It should be noted that the results from the preliminary experiments showed that the intensity values lower than the 75 %, the frequencies higher than 15 kHz and the scanning speed above 400 mm/s produce very low energy per unit area resulting in no ablation. On the other hand, the scanning speed lower than 25 mm/s, the pulse frequency less than 5 kHz and the pulse intensity higher than 96 % result in uncontrollable material removal due to an excessive increase in the energy per unit area and increase the dimensional errors and surface roughness. First set of experiments (36 runs) was executed for certain range of parameters (see Table 3) and the results showed that fabricated micro-channels were significantly oversized and acquire V-shape instead of designed shape i.e. square cross-section. Based upon the results of 36 experiments a new set of experiment was performed wherein the ranges of control factors were further fine-tuned and layer thickness per laser scan was increased from 2 μm to 4 μm per laser scan. Details of the experimentation including ranges of control factors are presented in Table 3.

Five responses regarding micro-channels geometry are selected for the analysis purpose including upper width (W_U), lower width (W_L), depth (D), taper angle at the right side (θ_R), and taper angle at the left side (θ_L). These responses were recorded from the microscopic images arranged for each of the individual micro-channel machined in zirconia oxide through laser beam machining and measuring the geometrical dimensions with the help of measurement suit of the microscope (Olympus BX51M). In addition to geometrical responses, one quality responses named as surface roughness (Ra) and surface morphology have also been selected in order to study the topography of the machining results. The surface roughness was measured at the bottom of the machined channels by using DekTakXT stylus profiler. The measurement was carried out as per ISO 4287 standard using the stylus profiler with scan speed 5 μm/sec having a resolution of 0.125 μm/pt by following the Gaussian regression. Three different positions were selected for measuring Ra, and the average of the collected readings was used for analysis. Surface morphology was carried out by using scanning electron microscope (SEM) from JEOL, Japan (Model JSM-7600F). Before SEM analysis, the machined samples were coated with platinum using JFC 1600 auto fine coater from JEOL Ltd to enhance their visibility during SEM analysis.

3. Results and discussion

Two sets of experimental runs were performed to fabricate square and rectangular cross-sectional micro-channels. First set consists of 36 experimental runs which were designed based on the combinations of three laser parameters naming laser intensity, pulse frequency and laser scanning speed each having four levels. The experimental results against each of the experimental runs are shown in Table 4. Likewise, the experimental results of 24 runs (2nd set of experimentation) are tabulated in Table 5. It is worth noting that two types of micro-channels have been achieved after laser machining. One type consists of micro-channels with a considerable amount of lower width (W_L) and the second type consists of zero lower width (W_L = 0) i.e.V-shaped. A schematic diagram is illustrated in Fig. 1 wherein all the five geometrical responses (W_U, W_L, D, θ_L and θ_R) are labelled. The quantitative results of square cross-sectional micro-channels shown in Table 4 reveal that the micro-channels produced against all the combinations of laser parameters were V-shaped except for few experimental runs. Thus, the lower width (W_L) of the channel is tabulated as 0. Since the bottom end of the channels was conical instead of the flat bottom. Therefore, the surface roughness of these channels were not considered into account.

Fig. 2 shows the optical microscopic images (taken at a magnification of 5X) of selected micro-channels (designed square cross-section) machined after laser machining. It can be seen that almost all the micro-channels are actually V-shaped and in each case, the depth of micro-channel is always greater than the designed depth of 500 μm. On the other end, the machining results of rectangular cross-sectional micro-channels are presented in Fig. 3. The images shown in Fig. 3 (taken at a magnification of 5X) reveals that the micro-channels are somehow closer to the designed geometry of rectangular cross-section. There is a considerable variation in the geometry of the micro-channels especially in case of depth

Table 4. Experimental results of 1st set of experiments (36 runs).

Exp. runs	Laser intensity; I (%)	Pulse frequency; f (kHz)	Scanning speed; v (mm/s)	Upper width; W_U (μm)	Lower width; W_L (μm)	Depth; D (μm)	Taper left; θ_L (deg)	Taper right; θ_R (deg)
1	75	5	25	685.9	0	1301	9.71	9.71
2	75	5	50	668.2	0	1186	10.5	6.84
3	75	5	75	654.9	0	986.7	9.63	11.5
4	75	5	100	623.9	0	734.5	10.2	11.1
5	75	10	25	699.1	0	876.1	12.6	13.4
6	75	10	50	659.3	0	800.9	13.2	13.7
7	75	10	75	659.3	0	765.5	16.4	12.8
8	75	10	100	623.9	0	738.9	13.7	12.8
9	80	10	25	694.7	0	1150	10.8	9.54
10	80	10	50	677	0	1022	10.9	13.9
11	80	10	75	650.5	0	955.3	12.9	11.3
12	80	10	100	628.3	0	898.2	12	12.8
13	80	5	50	668.2	0	1381	8.78	9.46
14	80	10	50	699.1	0	1049	8.13	10.4
15	80	15	50	668.2	0	898.2	12.2	13.3
16	80	20	50	663.7	0	880.5	15.2	17.1
17	75	15	75	646	0	588.5	16.8	16.4
18	80	15	75	637.2	0	818.6	14.7	13.7
19	85	15	75	632.8	0	973.5	13.5	12
20	90	15	75	628.3	0	1270	7.2	8.66
21	85	5	75	619.5	0	1274	7.53	9.2
22	85	10	75	654.9	0	1155	12.8	11.3
23	85	15	75	641.6	0	969	12.3	15.8
24	85	20	75	637.2	0	920.4	12.2	14.2
25	75	5	100	628.3	0	681.4	9.03	10.6
26	80	5	100	623.9	0	827.4	8.33	12.9
27	85	5	100	597.4	0	827.4	11.21	9.89
28	90	5	100	606.2	0	1434	6.74	5.39
29	75	5	75	646	0	977.9	11.7	10.8
30	75	10	75	646	0	725.7	16.6	12.5
31	75	15	75	637.2	0	584.1	13.2	9.36
32	75	20	75	619.5	0	575.2	12	14.2
33	75	20	25	661.4	0	703.5	13.2	8.85
34	80	20	25	668.2	0	1027	10.6	9.6
35	85	20	25	672.6	0	1283	9.26	8.13
36	90	20	25	654.9	0	1513	6.39	6.01

of the channel. Therefore, it was felt necessary to investigate the effect of laser parameters to understand the contribution of the variable parameters in controlling the micro-channels geometry.

Effects of each of the laser parameters used in this research are studied categorically for both the sets of experiments performed for square and rectangular cross-sectional micro-channels (36 and 24 experimental runs).

Fig. 4 shows the parametric effects on micro-channels geometrical aspects for the case of square cross-sectional micro-channels (1st set of experiments). The graphs shown in Fig. 4 are plotted in such a way that for each value of an input variable the mean of all the experiments performed against that value was calculated and a single point for a specific response was generated. Similarly, the means of all experimental results associated with each level of input variable were plotted against every individual response. For example, four levels of laser intensity are used, and four points are plotted in the graph for each response. In this way connecting Fig. 4(a) with the experimental results as tabulated in Table 4, it can be

Table 5. Experimental results of 2nd set of experiments (24 runs).

Exp. runs	Laser intensity; I (%)	Pulse frequency; f (kHz)	Scanning speed; v (mm/s)	Upper width; W_U (μm)	Lower width; W_L (μm)	Depth; D (μm)	Taper left; θ_L (deg)	Taper right; θ_R (deg)	Surface roughness; R_a (μm)
1	87	5	100	517.7	567	231.8	27	26	4.31
2	87	5	200	539.5	548	100.6	28	26.5	5.17
3	87	5	300	525.9	559	92.1	16.5	17	6.56
4	87	5	400	515	539	69.83	14	13	7.87
5	93	11	100	564	432	740.2	17	17	3.13
6	93	11	200	520.4	553	335.2	20	23	3.94
7	93	11	300	501.4	585	184.4	16	16.7	4.53
8	93	11	400	591.3	570	145.3	19.3	19.3	5.42
9	87	8	200	525.9	590	195.5	16.8	19.4	5.47
10	90	8	200	523.2	606	220.7	20.2	22.1	3.93
11	93	8	200	517.7	598	237.4	14	21	4.67
12	96	8	200	501.4	606	312.9	19.3	17	2.7
13	87	15	400	474.1	604	148	14.3	11.3	2.95
14	90	15	400	466	578	167	14	14.6	2.41
15	93	15	400	441.4	568	201.1	12	20	4.07
16	96	15	400	583.1	560	237.4	22	20	2.44
17	93	5	300	525.9	622	114.5	11	10	6.11
18	93	8	300	520.5	608	181.6	17	19	5.2
19	93	11	300	553.1	606	212.3	16	19	2.45
20	93	15	300	618.5	549	273.7	12.1	16.6	3.8
21	96	5	100	512.3	586	368.7	15.3	19..7	3.35
22	96	8	100	719.4	537	670.4	15	15	2.9
23	96	11	100	692.1	439	843.6	13.4	11.7	2.42
24	96	15	100	621.3	395	969.3	11.3	9	2.13

inferred that the all the levels of laser intensity (75, 80, 85 and 90 %) produces the channels having an upper width (W_U) with no significant difference irrespective to the laser intensity levels. Although all the channels have an upper width greater than the designed value of channel width (W = 500 μm) but their relative difference is not significant. On the other end, laser intensity directly influences the depth of the channel. Moreover, at an elevated temperature above the melting point, the thermal expansion of the material also occurs depending upon the thermal expansion coefficient of the irradiated material which is 10.7x10-6 K-1 for zirconia oxide as shown in Table 2. High laser intensity means that the energy of the laser per laser scan gets high as a result of which the rate of material melting per laser scan gets high and consequently high material removal occurs. For example, at 75 % laser intensity the recorded depth is ~700 μm whereas the depth of 1500 μm is observed when the laser intensity is reached to 90 % as can be seen in Fig. 4(a). Thus, with an increase in the intensity of the laser beam, the resulting depth also increases. The effect of laser intensity on the taperness of the micro-channels' sidewalls is also shown in the graph. However, this difference is not much clear on the set graphical scale. Therefore, the significance of laser parameters on the taperness of sidewalls (left taper; θ_L and right taper; θ_R) is discussed in the section of ANOVA results.

Effects of the pulse frequency of the laser beam are presented in Fig. 4(b). Change in pulse frequency of the laser beam does not affect the upper width (W_U). However, it inversely affects the depth of micro-channel as the pulse frequency increases the depth of the micro-channel decreases. For example, increasing the pulse frequency from 5 kHz to 20 kHz the depth of channel reduces from ~1400 μm to ~800 μm. It has also been observed that the scanning speed of the laser beam plays a vital role in controlling the geometry of the micro-channel while machining square cross-sectional channels. Low scanning speed allows the laser beam to interact with the substrate material for a more extended period as compared to the high scanning speed. As the time duration of the laser-material interaction increases, the more material is melted, and consequently, oversized machining occurs. The effects of scanning speed are shown in Fig. 4(c). It can be seen that high scanning speed (100 mm/s) gives relatively less oversizing of the micro-channels upper width (W_U = 600 μm) whereas low scanning speed (25 mm/s) produces wider micro-channels (W_U = 700 μm). This highly influential mechanism of the laser scanning speed is more severely observed for the

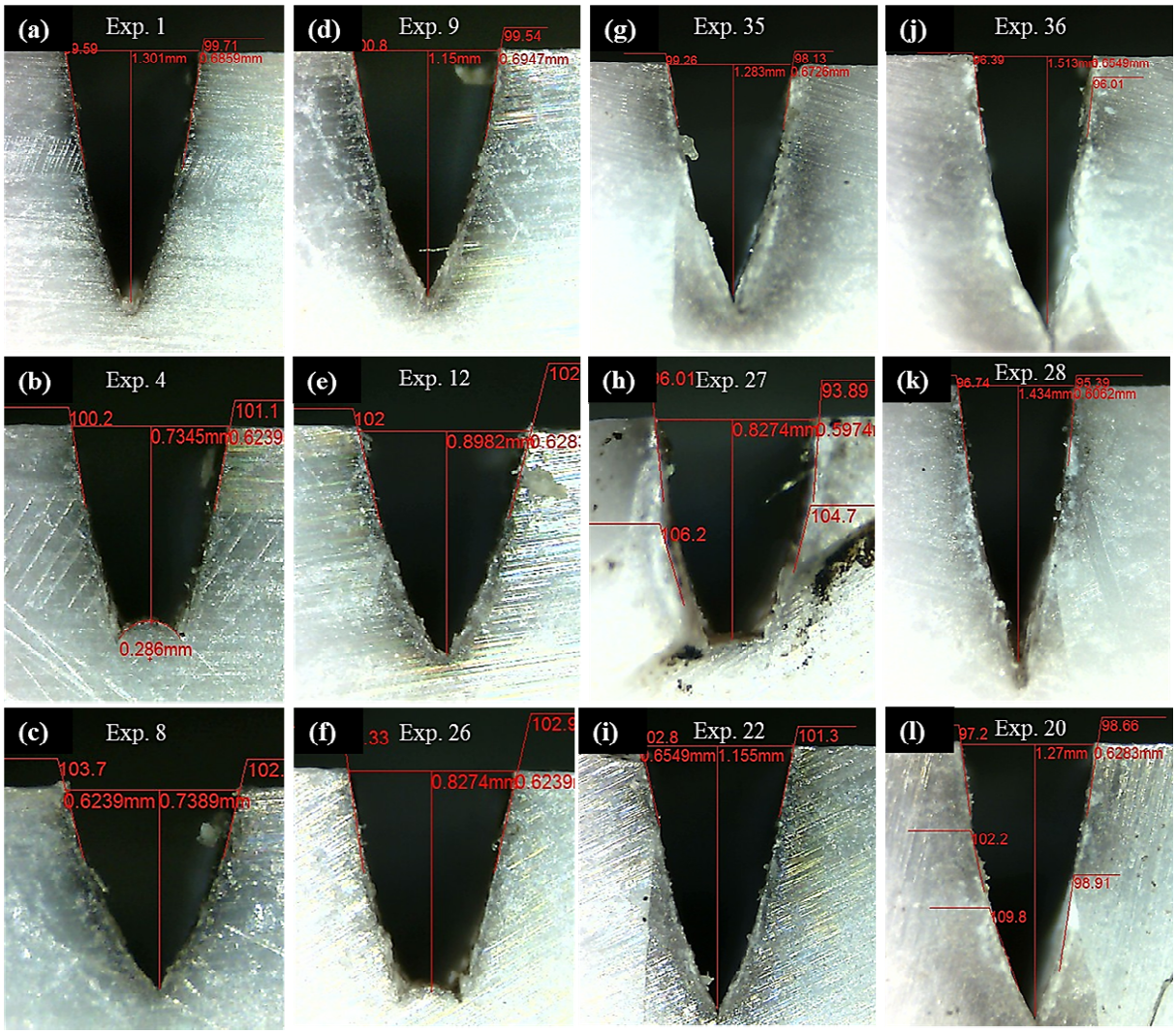

Fig. 2. Micro-channels machined under different machining conditions tabulated against experimental runs (1st set of experiments).

depth of channels. For example, a depth of ~700 µm is achieved against the scan speed of 100 mm/s and ~1300 µm depth (almost double depth) is resulted when the scanning speed was at its lowest level of 25 mm/s. These depths can also be evidenced by the micrographs presented in Figs. 2(a) and (b) where actual measurements of the dimensions are shown. Although, the resulted dimensions of the micro-channels are all oversized as compared to the designed dimensions (W = 500 µm and D = 500 µm), this set of experimentation played a significant role to understand the effects of laser parameters and to improve the laser parameters further as used for the 2nd set of experimentation.

The 2nd set of experiments was performed to fabricate the micro-channels of the rectangular cross-section of the designed width and depth of 500 µm and 800 µm, respectively. The selection of parameters was further improved based on the results obtained from the 1st set of experiments. Details of the improved levels and ranges of the control factors are shown in Table 3. The effects of laser parameters on the micro-channel geometry of rectangular cross-sectional micro-channels are shown in Fig. 5.

The effect of laser intensity on micro-channel geometry is shown in Fig. 5(a). Keeping the pulse frequency (f = 15 kHz) and scanning speed (v = 400 mm/s) at constant levels, the laser intensity directly influences the upper width and depth of micro-channel. A higher level of laser intensity (96 %) produces the channels with greater top width and depth. The upper width is ~600 µm, and depth is ~220 µm which is not as per designed dimensions.

The reason behind this variation is that since the scanning speed was kept at 400 mm/s, therefore, the time duration for laser-material interaction is insufficient to bring the irradiated work area at melting point and thus the desired amount of material layer to be removed is not fully melted. In this way, the material layer to be removed per laser scan was significantly less than the designed layer thickness of 4 µm. As a result, the machined depth is less compared to the anticipated depth of 800 µm. However, the graph helps us to understand

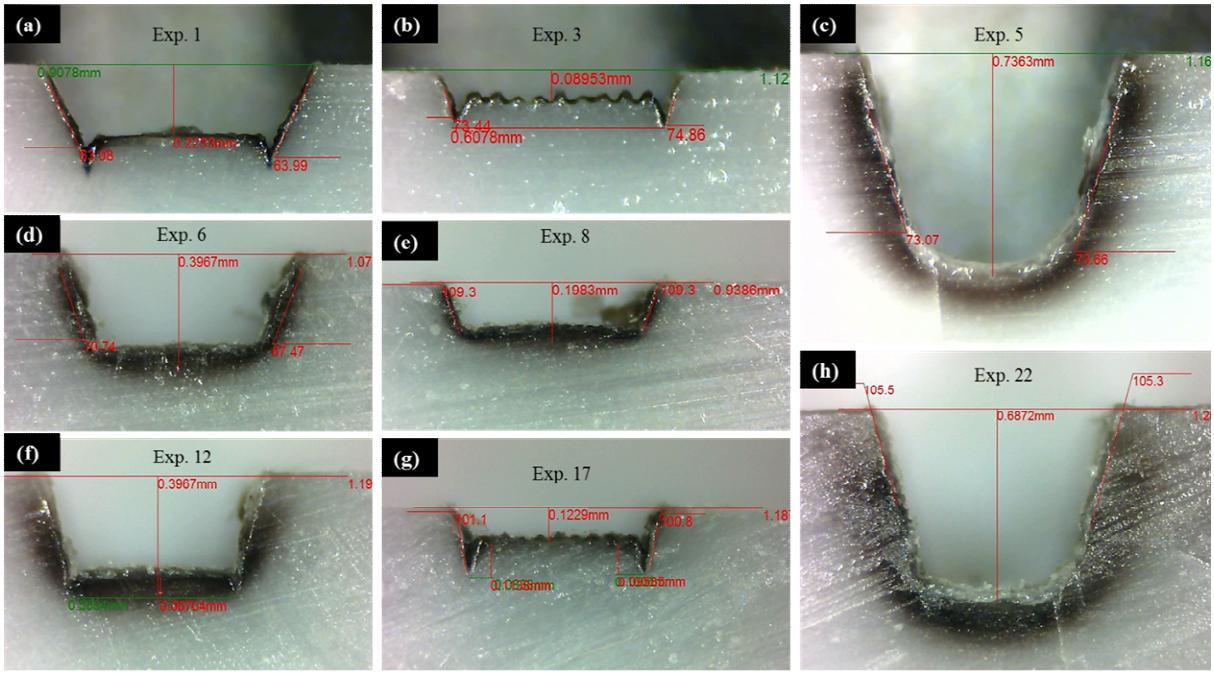

Fig. 3. Micro-channels machined under different machining conditions against experimental runs (2nd set of experiments).

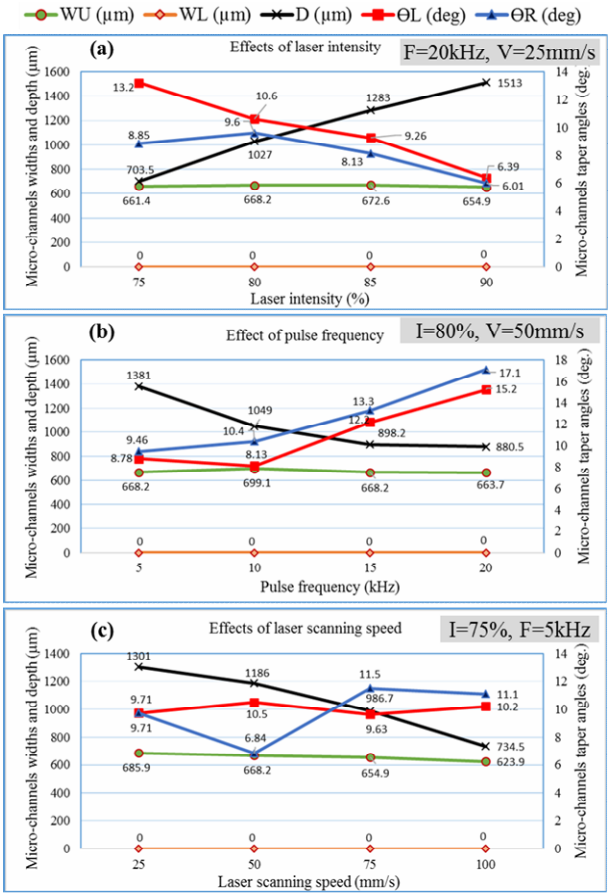

Fig. 4. Parametric effects during 1st set of experiments (36 runs).

the effect of laser intensity to capture the parametric trend. It is worth noting that the use of higher scanning speed range (100-400 mm/s) and high value of the layer thickness per laser scan (4 µm instead of 2 µm) allows the laser machining to generate micro-channels with a handful amount of lower width (W_L) of channel as can be seen from the micrographs shown in Fig. 3 for different experimental runs. For example, a lower width (W_L) of 600 µm can be achieved using laser intensity of 87 %, pulse frequency of 15 kHz and scanning speed of 400 mm/s (refer to Fig. 5(a)). Fig. 5(b) shows the trends of micro-channel geometry under the influence of pulse frequency while keeping other two parameters at their constant levels, i.e. I = 93 % and v = 300 mm/s. As the pulse frequency gets higher the micro-channels' upper width (W_U) also increases and reaches to above 600 µm at 15 kHz frequency which is an undesired trait of the machining. It is found that the lowest level of pulse frequency (f = 5 kHz) is more desirable if the upper width is wanted to be at 500 µm which is the designed value of upper width. Similarly, low pulse frequency generates micro-channel with greater lower width (W_L). Due to the presence of taper at both the sides of micro-channels, the lower width is always less than the designed width of 500 µm. Thus, the micro-channel wider at lower side is favourable to the machining objectives as we want to have the lower width as maximum as possible. Therefore, it can be extracted that the lower level of pulse frequency (5 kHz) can fulfil the laser machining requirements concerning upper and lower widths of micro-channels produced in zirconia oxide since it gives dimensions relatively closer to the designed dimensions. On the other end, low pulse frequency generates lesser depths. In order to get the deeper channels pulse frequency should be increased.

The effects of laser scanning speed are shown in Fig. 5(c) where the pulse frequency is kept at 5 kHz and laser intensity

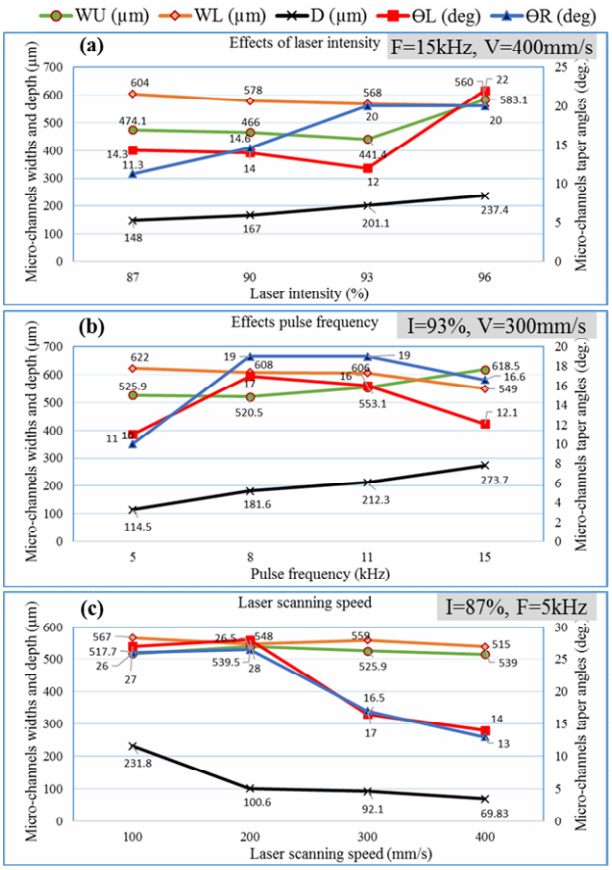

Fig. 5. Parametric effects during 2nd set of experiments (24 runs).

at 87 %. It can be seen that by varying the scanning speed there is no significant variation in micro-channel's upper and lower widths. However, the depth of channel is controlled by scanning speed. The lower level of scanning speed (100 mm/s) gives higher depths as compared to the high levels of scanning speed which generate the channels with less amount of depth.

The roughness of inner surface of the micro-channels are measured for the case of rectangular cross-sectional micro-channels. Channel width was considered as the cut-of-length. 2D graphical profile of the micro-channel along the vertical axis (y-axis) and its surface roughness measurement is shown in Fig. 6. Standard scan mode was adopted to get 2D profile of the micro-channel. Furthermore, two points are marked as R and M within which the roughness was measured regarding average Ra, Rt and Rz. A sample measurement data against one micro-channel is presented in the table affixed with Fig. 6. Since Ra is the most commonly used surface roughness parameter, therefore the roughness in terms of Ra is considered for analysis purposes. Additionally, a 3D profile is illustrated in Fig. 7 obtained through map scan mode of the stylus profiler. It shows the profiles along both the x- and y-axis.

The effects of laser parameters on the surface roughness are also studied in order to get trends of surface roughness against different laser parameters as shown in Fig. 8. The surface roughness results are based on the second set of experiments

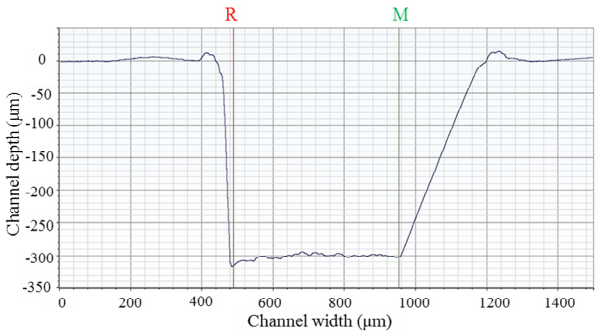

Label	Value	R Pos	R width	M Pos	M
Total Ra	3.05 µm	488.94 µm	0 µm	953.32 µm	0 µm
Total Rz	21.73 µm	488.94 µm	0 µm	953.32 µm	0 µm
Total Rt	21.73 µm	488.94 µm	0 µm	953.32 µm	0 µm

Fig. 6. A 2D graphical profile of surface roughness of inside base of micro-channel after laser machining.

shown in Table 5. It can be found that the surface roughness of the inner ground of the micro-channel is inversely proportional to the laser intensity and pulse frequency. Higher the laser intensity is the more is the pulse energy per laser spot which allows the substrate to be melted and removed in a more precise fashion. Due to the proper melting of the material under the action of high energy density, a more uniform layer of material is removed and leaving the surface with good quality (low surface roughness). Similar is the case for pulse frequency. High pulse frequency means that the number of pulses per laser spot/scan are greater which consequently increases the energy density and prepare the surface with low surface roughness. On the other end, the roughness of the laser machined surface of zirconia oxide is found to be directly proportional to the laser scanning speed. Scanning with high speed allows the laser beam to interact with the substrate for a shorter period causing insufficient time to the proper melting of the material. Insufficient melting causes the surface to be rough as compared to the case when the exact amount of melting occurs. The scan speed of 100 mm/s is observed to give minimum surface roughness of Ra 4.31 µm as compared to scan speed of 400 mm/s which produces a micro-channel surface having Ra 7.87 µm as can be seen from Fig. 8(c).

Analysis of variance (ANOVA) has been performed to identify the significance of each of the laser parameters with respect to each of the six individual responses. A confidence interval of 95 % (p-value = 0.05) is set for this analysis. ANOVA results obtained from the experimental results of 36 experimental runs are presented in Table 6. It can be found that the pulse frequency and laser scanning speed are the most significant factors affecting the upper width (W_U) of micro-channels. It has been inferred from the ANOVA results that all the three laser parameters (laser intensity, pulse frequency and scan speed) directly influence the depth (D), taper along left side (θ_L) and taper along right side (θ_R) of the micro-channel since all the parameters have p-value less than the reference value of 0.05. P-values of all the significant factors

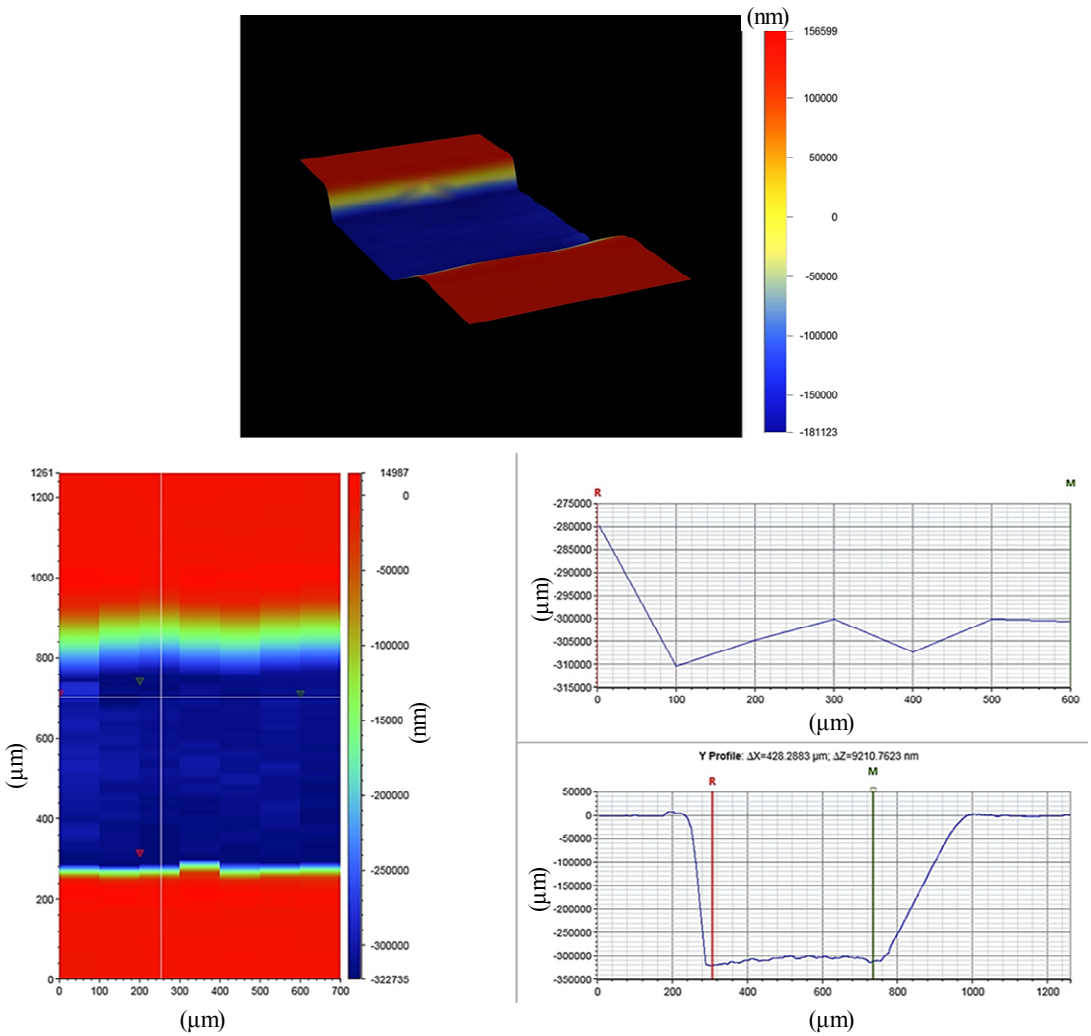

Fig. 7. A 3D graphical profile of surface roughness of inside base of micro-channel after laser machining.

concerning each response are shown in bold at last column of Table 6.

On the other end, the ANOVA results related to 2nd set of experiments (24 runs) are presented in Table 7. It should be noted that the 2nd set of experiments were performed using the refined parameters of the laser beam which mainly include the change in laser scanning speed (ranging within 100-400 mm/s) and layer thickness per laser scan (4 µm/scan instead of 2 µm/scan). The corresponding prominent difference in micro-channel geometry was to achieve micro-channels with a noticeable amount of lower width and a controlled depth. Therefore, the ANOVA results reflected accordingly in such a way that the significant factors were different in this case. For example, none of the laser parameters is significant if we talk about the upper width (W_U) of the micro-channel. Although the parameters affect the upper width but in an insignificant manner. The lower width (W_L) and depth (D) of micro-channel both are significantly affected by parametric values of pulse frequency and laser scanning speed. The trends of their effects can also be seen in Fig. 5. Although the manufactured channels have sides with certain taper but there is no factor among the selected factors which significantly affect the taper angle of the side walls of micro-channels. With reference to both the taper angles at left and right side (θ_L & θ_R), all the three laser parameters have p-values greater than the set value of 0.05 used for deciding the significance of a parameter. On average, a taper of 10-20 degrees has been found during the laser machining of zirconia oxide. The surface roughness of the laser machined micro-channels has been a response significantly affected by pulse frequency of the laser beam as well as the scanning speed of the laser scan.

Inside surface details of the micro-channels have been studied with the help of JEOL's scanning electron microscopic (SEM) images. Fig. 9 shows the selected images of the micro-channels produced in zirconia oxide through laser machining. Figs. 9(a) and (b) show the micro-channels obtained against the parametric combinations used in experimental runs of 15 and 16, respectively. Both the micro-channels are produced using laser intensity of 80 % and scanning speed of 50 mm/s. The difference is only in pulse frequency which was 15 kHz

Table 6. ANOVA results of 36 experimental runs (square micro-channels).

Responses	Source	Adj. SS	Adj. MS	F-value	p-value
Upper width; W_U (μm)	Regression	17306.2	5798.7	38.22	0.000
	Laser intensity; I (%)	701.8	701.8	4.65	0.390
	Pulse frequency; f (kHz)	660.4	660.4	4.38	**0.044**
	Scanning speed; v (mm/s)	14975.4	14975.4	99.21	**0.000**
	Lack-of-fit	4370.7	168.1	2.2	0.166
Depth; D (μm)	Regression	1788571	5961190	55.7	0.000
	Laser intensity; I (%)	1279647	1279647	119.56	**0.000**
	Pulse frequency; f (kHz)	553154	553154	51.68	**0.000**
	Scanning speed; v (mm/s)	697513	697513	65.17	**0.000**
	Lack-of-fit	339876	13072	29.88	0.000
Taper left; θ_L (deg)	Regression	126.50	42.165	10.07	0.000
	Laser intensity; I (%)	94.75	94.748	22.62	**0.000**
	Pulse frequency; f (kHz)	61.47	61.471	14.67	**0.001**
	Scanning speed; v (mm/s)	22.01	22.011	5.25	**0.029**
	Lack-of-fit	120.17	4.622	2.0	0.198
Taper right; θ_R (deg)	Regression	91.32	30.439	5.64	0.003
	Laser intensity; I (%)	51.02	51.019	9.45	**0.004**
	Pulse frequency; f (kHz)	51.06	51.062	9.46	**0.004**
	Scanning speed; v (mm/s)	37.31	37.307	6.91	**0.013**
	Lack-of-fit	134.16	5.160	0.8	0.684

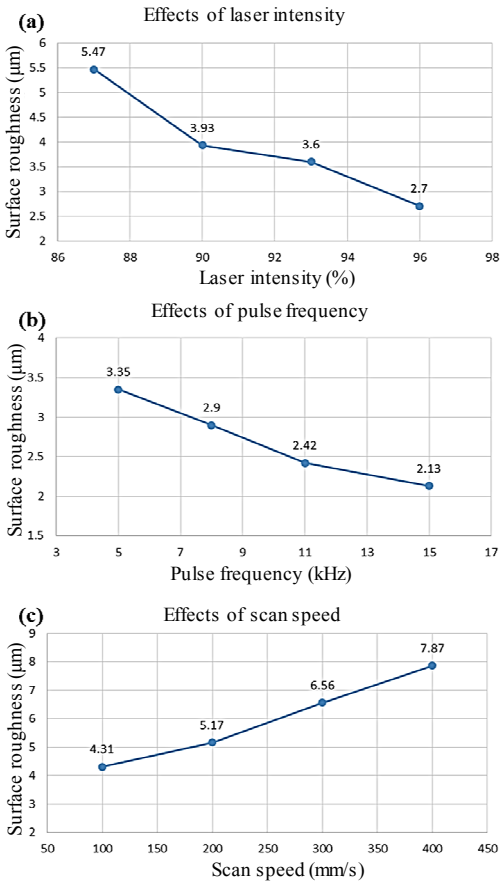

Fig. 8. Parametric effects on surface roughness.

during experimental run 15 and 20 kHz during experimental run 16. Enlarged views of both of these micro-channels reveal that the micro-channels are almost the same in quality concerning the edges and side walls. The edges of the channels are burr free, and the surfaces are well clean. It leads to the result that the change in pulse frequency contributes but insignificantly. It can also be seen that both the channels are V-shaped which is presumed to be the cause of the poor combination of laser intensity and scanning speed as the scanning speed was 50 mm/s in both of these cases allowing the laser beam to stay on for a relatively longer period and causes excessive melting. Layer thickness per laser scan was 2 μm/laser scan due to which energy density per laser spot per unit area gets concentrated and causes aggressive machining. As a result, the micro-channels' depth gets enlarged, and final geometry acquired V-shape. Presence of taper and excessive melting both contribute to getting deeper micro-channels than the anticipated depth. On the other end the channel shown in Fig. 9(c) is the result of 26th experiment run of the first set of experiments performed under the laser intensity of 80 %, pulse frequency of 5 kHz and scanning speed of 100 mm/s. Inside walls of the channels are not as clean as were in the previous two cases (Figs. 9(a) and (b)). There are some burrs at the edges. Sidewalls and the bottom surface of the channel are crowded with the molten material in the form of a re-solidified layer.

Under the first set of experiments, the machining was performed at low layer thickness (2 μm/laser scan) and low levels of scanning speed (25-100 mm/s). Low layer thickness per

Table 7. ANOVA results of 24 experimental runs (rectangular micro-channels).

Responses	Source	Adj. SS	Adj. MS	F-value	p-value
Upper width; W_U (μm)	Regression	338666.7	11288.9	3.45	0.036
	Laser intensity; I (%)	7786.6	7786.2	2.38	0.139
	Pulse frequency; f (kHz)	839.2	839.2	0.26	0.618
	Scanning speed; v (mm/s)	11349	11349	3.47	0.077
	Lack-of-fit	64161.1	3376.9	2.53	0.463
Lower width; W_L (μm)	Regression	34193.2	11397.7	5.19	0.008
	Laser intensity; I (%)	400.4	400.4	0.18	0.674
	Pulse frequency; f (kHz)	15717.8	15717.8	7.16	**0.015**
	Scanning speed; v (mm/s)	25445.6	25445.6	11.59	**0.003**
	Lack-of-fit	43684.3	2299.2	10.43	0.240
Depth; D (μm)	Regression	1126653	375551	28.44	0.000
	Laser intensity; I (%)	49853	49853	3.77	0.066
	Pulse frequency; f (kHz)	222512	222512	16.85	**0.001**
	Scanning speed; v (mm/s)	635016	635016	48.08	**0.000**
	Lack-of-fit	263739	13881	35.66	0.131
Taper left; θ_L (deg)	Regression	89.4	29.8	1.66	0.27
	Laser intensity; I (%)	34.3	34.3	1.92	0.182
	Pulse frequency; f (kHz)	9.5	9.5	0.53	0.474
	Scanning speed; v (mm/s)	12.4	12.4	0.70	0.414
	Lack-of-fit	358.5	18.8	0.96	0.516
Taper right; θ_R (deg)	Regression	58.8	19.6	0.89	0.465
	Laser intensity; I (%)	20.5	20.5	0.93	0.347
	Pulse frequency; f (kHz)	6.8	6.8	0.31	0.585
	Scanning speed; v (mm/s)	5.1	5.1	0.23	0.636
	Lack-of-fit	416.7	23.1	8.75	0.261
Surface roughness; R_a (μm)	Regression	37.602	12.5341	17.13	0.000
	Laser intensity; I (%)	1.653	1.6529	2.26	0.148
	Pulse frequency; f (kHz)	19.323	19.3234	26.42	**0.000**
	Scanning speed; v (mm/s)	9.281	9.2813	12.69	**0.002**
	Lack-of-fit	12.467	0.6561	0.30	0.915

laser scan allows the channels to be deeper than the required depth of channels (500 μm). The result was found to be the V-shaped micro-channels with almost zero value of lower width (W_L) instead of channels with flat lower width. That is why the 2nd set of experiments were executed under relatively high layer thickness (4 μm/lase scan) and higher levels of scanning speed (100-400 mm/s). Selected SEM images of the machined channels are shown in Fig. 10 showing that the micro-channels with flat lower widths are possible to achieve using higher levels of layer thickness and scanning speed. Fig. 10(a) shows three micro-channels produced under the laser parametric combinations against experimental runs 11, 12 and 13. The details of laser parameters can be seen in Table 5. An enlarged view of micro-channel produced during experimental run 12 is shown in Fig. 10(b) showing that the micro-channels' edges are equipped with the spatter ejected after melting and re-solidified at the edges. However, the surface roughness of the bottom face of micro-channel is relatively good (R_a = 2.7 μm). Since this channel was produced using laser intensity 96 %, pulse frequency 8 kHz and scanning speed 200 mm/s, so the corresponding depth was recorded ~ 312 μm whereas the next channel was shallower in depth (D ~148 μm) just because the machining was conducted at higher scanning speed (400 mm/s) and low laser intensity (86 %). It means that the material removal per laser scan was less than 4 μm. Thus, it can be stated that the laser beam should be in contact with the substrate surface for an appropriate period and the intensity of laser should be high enough to remove the required layer of material per laser scan after the accurate amount of material melting. Otherwise, the laser beam would be able to perform partial melting underneath the laser spot. It can be evidenced by Fig. 10(d) presenting the enlarged view of micro-channel associated with experimental run 17 which is performed with 93 % laser intensity, 5 kHz pulse frequency and 300 mm/s scanning speed. The resulted depth was recorded just as 114.5 μm which is expected to be the cause of improper time

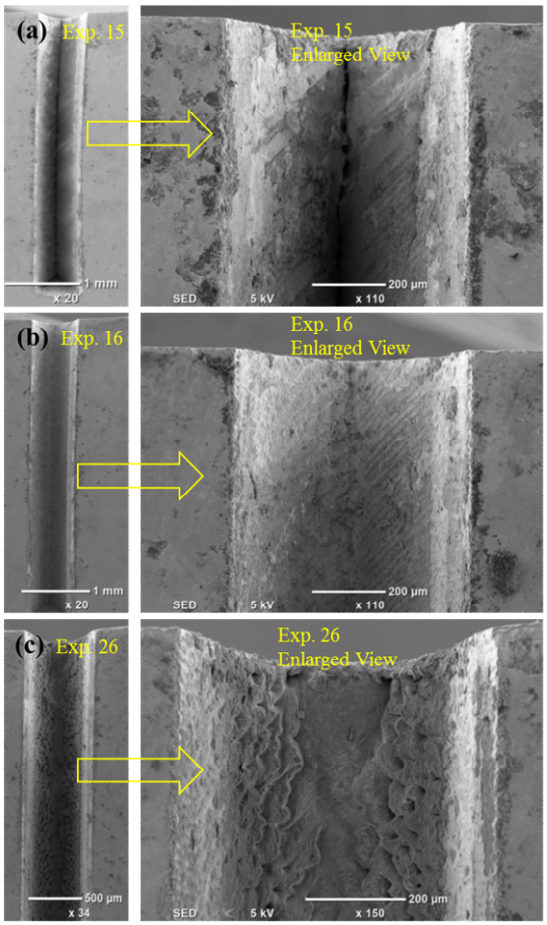

Fig. 9. SEM analysis of micro-channels machined under different machining conditions against experimental runs performed during 1st set of experiments: (a) Exp. 15; (b) exp.16; (c) exp. 26.

available for the laser beam due to high scan speed.

The resultant surface texture at the bottom face of micro-channel is found to be like small drops spread longitudinally along the channel length. The main cause is the insufficient melting. That is why the roughness recorded for this micro-channel was relatively high, i.e. R_a = 6.11 µm. SEM images of experimental runs 21, 22 and 23 are shown in Fig. 10(e) all performed using laser intensity 96 %, scanning speed 100 mm/s and pulse frequency 5 kHz, 8 kHz and 11 kHz, respectively. Due to the appropriate combination of laser parameters (high intensity; 96 %, moderate scanning speed; 100 mm/s and relatively high layer thickness; 4 µm/laser scan), it was anticipated that the resulting depths of micro-channels would be closer to the designed depth of 800 µm. The actual machining results were significantly meeting the geometrical expectations. For example, the depths against the above said three experiments were 368 µm, 670 µm and 843 µm, respectively, revealing that an increase in pulse frequency positively contribute in building depth of micro-channel. A similar observation has been noticed concerning the surface roughness of the machined channel. For example, the surface roughness (R_a values) against the said experimental runs (21, 22 and 23) are 3.35 µm, 2.9 µm and 2.42 µm, respectively. Even by a further increase in frequency, i.e. 15 kHz, the surface roughness was R_a 2.13 µm. The corresponding SEM images of the said three experimental runs are shown in Fig. 10(e) highlighting that the inside surface integrity of the micro-channels is quite smooth. An enlarged view is shown in Fig. 10(f) exhibiting that the inside surface of the micro-channel is free from any re-solidification of the molten debris leaving the surface with a roughness of R_a 2.9 µm.

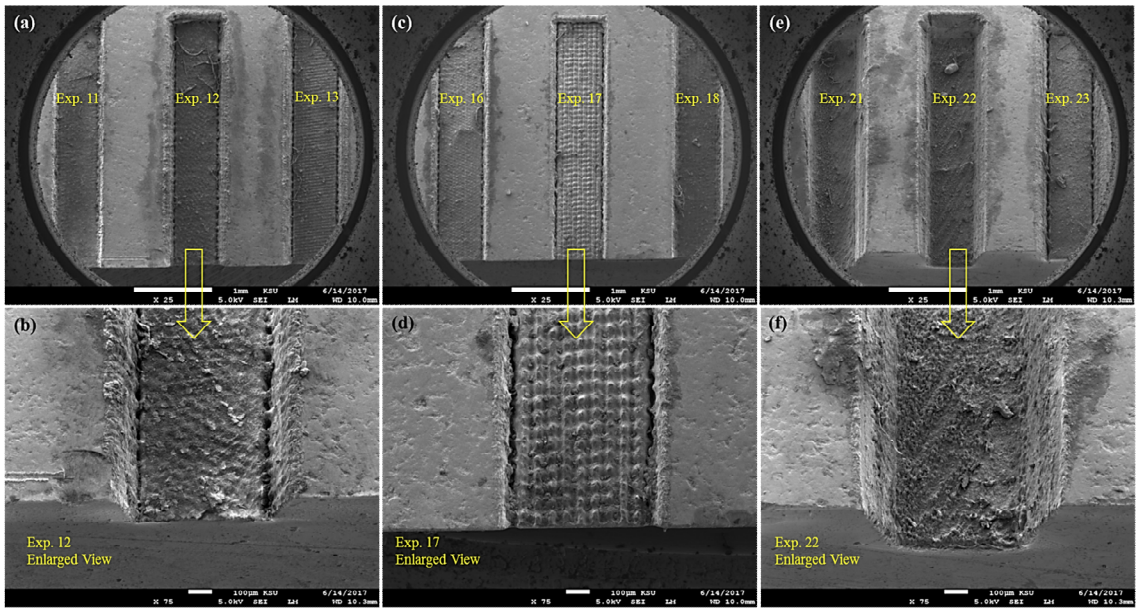

Fig. 10. Scanning electron microscopic analysis of micro-channels machined under different machining conditions against experimental runs performed during 2nd set of experiments: (a) Exp. 11-13; (b) enlarged view of exp.12; (c) exp. 16-18; (d) enlarged view of exp. 17; (e) exp. 21-23; (f) enlarged view of exp. 22.

4. Conclusions

Micro-channels have been fabricated in dental Yttria stabilized zirconia oxide through laser beam machining. Performance of laser machining has been evaluated regarding geometrical characteristics of micro-channels including width, depth and taper angles of sidewalls. The quality of micro-channels is further studied though SEM analysis and surface roughness of the inner machined surfaces of the micro-channels. Based on the experimental results, discussion, ANOVA and SEM analysis, the following conclusions could be inferred:

(1) The geometry of the resulting micro-channels in zirconia through laser machining is very sensitive to the slight variation in laser parameters. High values of laser intensity (> 90 %) along with lower levels of scanning speed (< 100 mm/s) causes the laser beam to produce deeper V-shaped micro-channels. On the contrary, scanning speed ≥ 100 mm/s allows the laser beam to interact with the substrate for a reasonable period and consequently produces U-shaped micro-channels. However, a taper angle of 10-20^{o} could not be avoided in any case.

(2) All the laser parameters including laser intensity, pulse frequency, scanning speed and layer thickness are found to be significant controlling factors for different responses. However, it is found that the layer thickness per laser scan has a direct influence on the geometry of the machined channels. Almost all the micro-channels are found to be V-shaped by using a layer thickness of 2 μm/laser scan. A layer thickness of 4 μm per laser scan is found to be more suitable to achieve micro-channels with geometrical dimensions closer to the designed dimensions.

(3) Surface quality of the machined micro-channels is found to be encouraging since the micro-channels with Ra value of ~ 2 μm can be achieved. Higher levels of laser intensity (96 %), pulse frequency (15 kHz) and lower levels of scanning speed (100 mm/s) allowed to achieve clean and burr-free micro-channels with good surface roughness.

Acknowledgments

The authors extend their appreciation to the Deanship of Scientific Research at King Saud University for funding this work through research group No (RG-1439-009).

References

[1] S. Xu, Z. Yao and M. Zhang, Material removal behavior in scratching of zirconia ceramic surface treated with laser thermal shock, *Int. J. Adv. Manuf. Technol.,* 85 (9-12) (2016) 2693-2701.

[2] K. Oblov et al., Fabrication of microhotplates based on laser micromachining of zirconium oxide, *Phys. Procedia,* 72 (Supplement C) (2015) 485-489.

[3] R. Jafari et al., Modeling and analysis of surface roughness of microchannels produced by μ-WEDM using an ANN and Taguchi method, *J. Mech. Sci. Technol.,* 31 (11) (2017) 5447-5457.

[4] D. S. Oh et al., Effect of capillary action on bone regeneration in micro-channeled ceramic scaffolds, *Ceram. Int.,* 40 (7, Part A) (2014) 9583-9589.

[5] D. S. Oh et al., Bone marrow absorption and retention properties of engineered scaffolds with micro-channels and nano-pores for tissue engineering: A proof of concept, *Ceram. Int.,* 39 (7) (2013) 8401-8410.

[6] H.-J. Hong, S. K. Sarkar and B.-T. Lee, Formation of TiO_2 nano fibers on a micro-channeled Al_2O_3-ZrO_2/TiO_2 porous composite membrane for photocatalytic filtration, *J. Eur. Ceram. Soc.,* 32 (3) (2012) 657-663.

[7] K. Kowsari et al., CFD-aided prediction of the shape of abrasive slurry jet micro-machined channels in sintered ceramics, *Ceram. Int.,* 42 (6) (2016) 7030-7042.

[8] A. Banu, M. Y. Ali and M. A. Rahman, Micro-electro discharge machining of non-conductive zirconia ceramic: Investigation of MRR and recast layer hardness, *Int. J. Adv. Manuf. Technol.,* 75 (1-4) (2014) 257-267.

[9] P. Hou et al., Influence of open-circuit voltage on high-speed wire electrical discharge machining of insulating Zirconia, *Int. J. Adv. Manuf. Technol.,* 73 (1-4) (2014) 229-239.

[10] Y. Guo et al., Multi-response optimization of the electrical discharge machining of insulating zirconia, *Mater. Manuf. Process.,* 32 (3) (2017) 294-301.

[11] S. Sun, M. Brandt and M. Dargusch, Review of laser assisted machining of ceramics, *Zhongguo Jiguang/Chinese J. Lasers,* 36 (12) (2009) 3299-3307.

[12] J. Kim and B. Kang, Machining characteristics of micro lens mold in laser-assisted micro-turning, *J. Mech. Sci. Technol.,* 32 (4) (2018) 1769-1774.

[13] T.-W. Kim and C.-M. Lee, A study on the development of milling process for silicon nitride using ball end-mill tools by laser-assisted machining, *Int. J. Adv. Manuf. Technol.,* 77 (5-8) (2015) 1205-1211.

[14] J. Do Kim, S. J. Lee and J. Suh, Characteristics of laser assisted machining for silicon nitride ceramic according to machining parameters, *J. Mech. Sci. Technol.,* 25 (4) (2011) 995-1001.

[15] T. Kizaki et al., Laser-assisted machining of zirconia ceramics using a diamond bur, *Procedia CIRP,* 42 (Supplement C) (2016) 497-502.

[16] S. Xu et al., An experimental investigation of grinding force and energy in laser thermal shock-assisted grinding of zirconia ceramics, *Int. J. Adv. Manuf. Technol.,* 91 (9-12) (2017) 3299-3306.

[17] J. P. Parry et al., Nanosecond-laser postprocessing of millisecond- laser-machined zirconia (Y-TZP) surfaces, *Int. J. Appl. Ceram. Technol.,* 5 (3) (2008) 249-257.

[18] F. C. Dear et al., Pulsed laser micromachining of yttria‐stabilized zirconia dental ceramic for manufacturing, *Int. J. Appl. Ceram. Technol.,* 5 (2) (2008) 188-197.

[19] A. N. Samant and N. B. Dahotre, Absorptivity transition in

the 106 μm wavelength laser machining of structural ceramics, *Int. J. Appl. Ceram. Technol.,* 8 (1) (2011) 127-139.

[20] J. P. Parry et al., Laser micromachining of zirconia (Y-TZP) ceramics in the picosecond regime and the impact on material strength, *Int. J. Appl. Ceram. Technol.,* 8 (1) (2011) 163-171.

[21] M. Noda et al., Surface damages of zirconia by Nd:YAG dental laser irradiation, *Dent. Mater. J.,* 29 (5) (2010) 536-541.

[22] S. Guarino et al., Laser milling of yttria-stabilized zirconia by using a Q-switched Yb:YAG fiber laser: experimental analysis, *The International Journal of Advanced Manufacturing Technology*, 94 (1-4) (2018) 1373-1385.

[23] H. D. Vora et al., One-dimensional multipulse laser machining of structural alumina: Evolution of surface topography, *Int. J. Adv. Manuf. Technol.,* 68 (1-4) (2013) 69-83.

[24] M. K. Mohammed and U. Umer, Optimization of laser micro milling of alumina ceramic using radial basis functions and MOGA-II, *The International J. of Advanced Manufacturing Technology* (2017) 2017-2029.

[25] H. Vora and N. Dahotre, Laser machining of structural alumina: influence of moving laser beam on the evolution of surface topography, *Int. J. Appl. Ceram. Technol.,* 12 (3) (2015) 665-678.

[26] *CeramTec - The Ceramic Experts*.

[27] B. M. A. Abdo et al., Laser micro-milling of bio-lox forte ceramic: An experimental analysis, *Precis. Eng.,* 53 (April) (2018) 179-193.

[28] B. M. A. Abdo et al., Experimental investigation and multi-objective optimization of Nd:YAG laser micro-channeling process of zirconia dental ceramic, *Int. J. Adv. Manuf. Technol.,* 98 (2018) 1-18.

[29] Y. Liu et al., Fabrication of micro-scale textured grooves on green ZrO_2 ceramics by pulsed laser ablation, *Ceram. Int.,* 43 (8) (2017) 6519-6531.

[30] C. Leone et al., Experimental investigation on laser milling of aluminium oxide using a 30 W Q-switched Yb: YAG fi ber laser, *Opt. Laser Technol.,* 76 (2016) 127-137.

Basem M. A. Abdo is a researcher at Advanced Manufacturing Institute, King Saud University, Riyadh, Saudi Arabia. He received M.Sc. degree in industrial engineering from King Saud University in 2013. His research interests mainly include advanced manufacturing technologies; micro-machining, CAD/CAM, optimization of manufacturing processes.